JB Journals.ASM.org

# Comparative Analysis of *kdp* and *ktr* Mutants Reveals Distinct Roles of the Potassium Transporters in the Model Cyanobacterium *Synechocystis* sp. Strain PCC 6803

**Kei Nanatani,[a] Toshiaki Shijuku,[a] Yousuke Takano,[a] Lalu Zulkifli,[a]* Tomoko Yamazaki,[b] Akira Tominaga,[a] Satoshi Souma,[a] Kiyoshi Onai,[c] Megumi Morishita,[c] Masahiro Ishiura,[c] Martin Hagemann,[d] Iwane Suzuki,[e] Hisataka Maruyama,[f] Fumihito Arai,[f] Nobuyuki Uozumi[a]**

Department of Biomolecular Engineering, Graduate School of Engineering, Tohoku University, Sendai, Japan[a]; School of Agricultural Sciences, Nagoya University, Nagoya, Japan[b]; Center for Gene Research, Nagoya University, Nagoya, Japan[c]; Department of Plant Physiology, University of Rostock, Rostock, Germany[d]; Faculty of Life and Environmental Sciences, University of Tsukuba, Ibaraki, Japan[e]; Department of Micro-Nano Systems Engineering, Graduate School of Engineering, Nagoya University, Nagoya, Japan[f]

**Photoautotrophic bacteria have developed mechanisms to maintain $K^+$ homeostasis under conditions of changing ionic concentrations in the environment. *Synechocystis* sp. strain PCC 6803 contains genes encoding a well-characterized Ktr-type $K^+$ uptake transporter (Ktr) and a putative ATP-dependent transporter specific for $K^+$ (Kdp). The contributions of each of these $K^+$ transport systems to cellular $K^+$ homeostasis have not yet been defined conclusively. To verify the functionality of Kdp, *kdp* genes were expressed in *Escherichia coli*, where Kdp conferred $K^+$ uptake, albeit with lower rates than were conferred by Ktr. An on-chip microfluidic device enabled monitoring of the biphasic initial volume recovery of single *Synechocystis* cells after hyperosmotic shock. Here, Ktr functioned as the primary $K^+$ uptake system during the first recovery phase, whereas Kdp did not contribute significantly. The expression of the *kdp* operon in *Synechocystis* was induced by extracellular $K^+$ depletion. Correspondingly, Kdp-mediated $K^+$ uptake supported *Synechocystis* cell growth with trace amounts of external potassium. This induction of *kdp* expression depended on two adjacent genes, *hik20* and *rre19*, encoding a putative two-component system. The circadian expression of *kdp* and *ktr* peaked at subjective dawn, which may support the acquisition of $K^+$ required for the regular diurnal photosynthetic metabolism. These results indicate that Kdp contributes to the maintenance of a basal intracellular $K^+$ concentration under conditions of limited $K^+$ in natural environments, whereas Ktr mediates fast potassium movements in the presence of greater $K^+$ availability. Through their distinct activities, both Ktr and Kdp coordinate the responses of *Synechocystis* to changes in $K^+$ levels under fluctuating environmental conditions.**

Living cells have developed specific responses to hyperosmotic shock. Upon exposure to this stress, cells initially lose water and their volume shrinks. In all living cells, $K^+$ is the major intracellular cation used for the maintenance of turgor pressure, cytosolic osmolarity, protein structuring, and membrane potential (1–3). In contrast to animals, $Na^+/K^+$ ATP pumps are generally missing in bacteria and plants. Hence, these cells possess $K^+$ uptake transporters to supply $K^+$ to the cells. Particularly after hyperosmotic stress, cells quickly take up $K^+$ from the medium to increase the intracellular osmolarity, which prevents water efflux from the cell. Data from genetic and biochemical experiments indicate that the activity and the expression of these transporters respond to hyperosmotic stress. In the later phase of acclimation to hyperosmotic stress, cells also induce the synthesis of osmoprotective molecules, such as glutamate, trehalose, proline, and glucosylglycerol (4, 5). Despite an increasing amount of data on cellular osmoregulation involving ion flux across the membrane, direct evidence for the involvement of specific transporters in the cellular response to osmotic up-shock is lacking for photoautotrophic organisms.

The cyanobacterium *Synechocystis* sp. strain PCC 6803 (hereinafter referred to as *Synechocystis*) is a frequently used unicellular photosynthetic prokaryote that can survive under a wide range of environmental conditions (6). Unlike *Escherichia coli*, *Synechocystis* possesses an internal thylakoid membrane system, which is mainly involved in photosynthesis. Based on their membrane structure and the nature of their selective $K^+$ filters, prokaryotes express three families of $K^+$ uptake transporters, Ktr/Trk/HKT, Kup/HAK/KT, and Kdp (7–12). Genes encoding proteins of the Kup family are absent from the *Synechocystis* genome, while it contains the $K^+$ transporter homologs Ktr and Kdp, as well as the characterized $K^+$ channels SynK and SynCaK (13–16). Previous studies have shown that the Ktr system is essential for the acclimation of the *Synechocystis* cell to osmotic stress caused either by ionic compounds like NaCl or by nonionic compounds like sor-

**Received** 4 September 2014 **Accepted** 9 October 2014

**Accepted manuscript posted online** 13 October 2014

**Citation** Nanatani K, Shijuku T, Takano Y, Zulkifli L, Yamazaki T, Tominaga A, Souma S, Onai K, Morishita M, Ishiura M, Hagemann M, Suzuki I, Maruyama H, Arai F, Uozumi N. 2015. Comparative analysis of *kdp* and *ktr* mutants reveals distinct roles of the potassium transporters in the model cyanobacterium *Synechocystis* sp. strain PCC 6803. J Bacteriol 197:676–687. doi:10.1128/JB.02276-14.

**Editor:** J. P. Armitage

Address correspondence to Nobuyuki Uozumi, uozumi@biophy.che.tohoku.ac.jp.

* Present address: Lalu Zulkifli, Department of Biology, Faculty of Technology and Training and Education, Mataram University, Mataram, Indonesia.

Supplemental material for this article may be found at http://dx.doi.org/10.1128/JB.02276-14.



doi:10.1128/JB.02276-14

bitol (17, 18). Recent studies of the transcription levels of *ktr* and *kdp* in *Staphylococcus aureus* revealed that both transporters are active systems in the acclimation to salt stress (19, 20). The results of these studies indicate that the Ktr system plays the dominant role in the accumulation of $K^+$ as a quick response to hyperosmotic shock.

In *E. coli*, the $K^+$ refill at high osmolality is performed by the Kdp transporter, a P-type ion-translocating ATPase that has been characterized in great detail (7, 21–25). Kdp is an inducible $K^+$ uptake system with high affinity and specificity for $K^+$ (24, 26). It consists of four subunits that are encoded by the *kdpFABC* operon in *E. coli*. KdpA binds and transports $K^+$, and KdpB catalyzes the hydrolysis of ATP in cooperation with KdpC. The gene products of the *kdpDE* operon have a regulatory role and form a typical two-component system (26). The tandem gene arrangement of two-component system and *kdp* operon was also found in *Staphylococcus aureus* (19, 27). The Kdp system functions as an emergency $K^+$ uptake system that is only expressed when the cell experiences osmotic stress or $K^+$ limitation and becomes rapidly degraded when no longer required (28). In *Synechocystis*, the homologous Kdp proteins are encoded by the *kdpABGCD* operon. KdpA is predicted to be a membrane protein containing $K^+$-conducting-pore regions (8). Growth tests using a *kdpA* mutant showed that, in *Synechocystis*, KdpA seems to play only a minor role in $K^+$ uptake compared to the role of the Ktr-type transporter (17). The regulatory two-component system of the *Synechocystis* Kdp has a different arrangement than the well-characterized situation in *E. coli*, since the histidine kinase KdpD seems to be split into two separate parts. The same situation has been observed in the desiccation-tolerant strain *Anabaena* sp. strain L-31 (28). In contrast to *Synechocystis*, this cyanobacterial strain harbors two operons encoding components of Kdp. Only one of these operons also includes a gene for the truncated KdpD. Thus, various compositions of the two-component system of Kdp have been found in bacteria.

Osmoadaptation of cells, including cyanobacterial cells, to external hyperosmotic shock entails solute flux across the plasma membrane that causes the sequential cell volume changes (4, 29). Conventional experimental batch culture approaches provide an average of many individual responses from many different cells, some of which may not actually undergo osmoadaptation. In this study, to dissect the individual contributions of the Ktr and Kdp transport systems under rapidly changing environmental conditions, we developed a microfluidic device that can be used to monitor discrete dynamic processes in single cells in real time. These studies revealed the minor importance of *kdp* in acclimation to hyperosmotic stress. Therefore, we characterized the *kdp* operon of *Synechocystis* in more detail, studied its circadian expression, and determined the physiological functions of Ktr and Kdp by heterologous expression in *E. coli*, as well as through analysis of *Synechocystis* mutants.

## MATERIALS AND METHODS

**Cells and growth conditions.** *Synechocystis* sp. strain PCC 6803 and mutant cells were grown at 30°C in BG11 medium containing 20 mM TES-KOH (pH 8.0) (18). Solid medium consisted of BG11 medium buffered at pH 8.0, 1.5% agar or agarose, and 0.3% sodium thiosulfate. Continuous illumination was provided by fluorescent lamps (50 μmol photons $m^{-2}$ $s^{-1}$ at 400 to 700 nm). Transformants of *E. coli* strain LB2003 ($F^-$ *thi lacZ gal rha* Δ*kdpFABC5 trk*Δ*1* Δ*trkA*) were cultured in a medium consisting of 1% tryptone, 0.5% yeast extract, 30 mM KCl, 1% glucose, 0.25 mM isopropyl-β-D-thiogalactopyranoside (IPTG), and the required antibiotics at 30°C (30).

**Microfluidic analysis.** The microfluidic device consisted of a coverslip made of polydimethylsiloxane (PDMS) and hydrogel cages on a glass slide. The coverslip was produced by replica molding with a master mold fabricated by photolithography. The positive-type photoresist (OFPR-800; Tokyo Ohka Kogyo) was spin coated onto the silicon wafer (1,000 rpm, 20 s), prebaked at 90°C for 15 min, and irradiated by UV light (405-nm wavelength) using a mask aligner (MA6; SÜSS MicroTec AG). Then, the UV-irradiated area of the photoresist was removed with NMD-3 reagent (Tokyo Ohka Kogyo) and rinsed with deionized water. The final thickness of the photoresist was 2 μm. The developed pattern was baked at 145°C for 30 min for hardening and used as a master mold for the following steps. The PDMS (Silpot 184 and its catalyst; Toray) was poured into the master mold and hardened in an oven at 90°C for 15 min. Then, the PDMS replica was peeled from the master mold. For the connections with tubing and a syringe pump, holes were made on the patterned PDMS coverslip. The hydrogel cages on the glass were produced by photolithography. Glass was preheated at 145°C for 10 s and then the 4.0% (wt/vol) photo-cross-linkable polymer (azide-unit pendant water-soluble photopolymer [AWP]; Toyo Gosei) was spin coated (500 rpm for 10 s) onto the glass, baked at 65°C for 20 min, and irradiated by UV light with photomask using the mask aligner to harden the photo-exposed AWP. The resulting hydrogel cages on the glass were cleaned with deionized water. The thickness of the hydrogel was 2 to 2.5 μm. Then, the PDMS coverslip and the hydrogel cages on the glass were connected by plasma treatment (plasma ion bombarder PIB-10; Vacuum Device), followed by heat treatment on a hot plate at 120°C to seal them completely. Cells in the hydrogel cages were observed with a charge-coupled device (CCD) camera (WAT-221S; Watec) through an objective lens (UPLSAPO 100XO, numeric aperture 1.4; Olympus). Simulation of the flow was performed according to the finite element algorithm using COMSOL analysis software (COMSOL, Inc., Palo Alto, CA). To set up the experiment, a *Synechocystis* cell was transported into the patterned hydrogel cage through in-port(a) at a flow rate of 300 μl/h, established by using a syringe pump. Determination of cell volume during hyperosmotic stress was performed by using Image J (NIH; http://rsb.info.nih.gov/ij/index.html) to measure the cell area, followed by converting area into volume under the assumption that the volume change was isotropic.

***E. coli* complementation assay.** The *Synechocystis kdpABGCD* (*slr1728* to *slr1729*, *ssr2912*, and *slr1730* to *slr1731*) region was amplified by PCR using the SacI site-containing forward primer, 5′-CAGTGAGCTCA TGTTGCAAGGTTTTG-3′, and the PstI site-containing reverse primer, 5′-CAGTCTGCAGTTAGCCATTGGCAATGA-3′, with *Synechocystis* genomic DNA as the template. The PCR fragment was digested with SacI and PstI and ligated into the corresponding sites of plasmid pPAB404 (31, 32). pSTV28-*ktrA* and pPAB404-*ktrEB* were used to express the Ktr $K^+$ transport system in *E. coli* (18). *E. coli* strain LB2003, which lacks the three $K^+$ uptake systems Trk, Kup, and Kdp (31) was used: LB2003 cells containing the empty vectors pSTV28 and pPAB404 or pSTV28-*ktrA* and pPAB404-*ktrEB* or the empty vectors or pSTV28 and pPAB404-*kdpABGCD* were grown in synthetic medium [46 mM $Na_2HPO_4$, 23 mM $NaH_2PO_4$, 8 mM $(NH_4)_2SO_4$, 0.4 mM $MgSO_4$, 6 μM $FeSO_4$, 10 μg/ml thiamine, 1% glucose, 1.2% agarose] (18) in the presence of 30 mM KCl, 0.25 mM IPTG, 25 μg/ml of ampicillin, and/or 15 μg/ml of chloramphenicol for 24 h at 30°C. Then, these precultures were washed with synthetic medium without KCl and diluted to an optical density at 600 nm ($OD_{600}$) of 0.005 with the same medium. Tenfold serial dilutions were plated on synthetic agar medium containing 7.5, 10, 15, or 20 mM KCl and incubated for 2 days at 30°C to test for growth. For growth curves, *E. coli* LB2003 cells expressing *ktr* or *kdp* were grown in synthetic medium containing 15 mM KCl.

**Measurement of $K^+$ uptake in *E. coli*.** $K^+$ influx was measured essentially as described previously (18, 33, 34). The net uptake of $K^+$ was mea-

sured by the silicone filtration technique, and the $K^+$ contents of the cell pellets were determined by flame photometry.

**Construction of *Synechocystis kdpA* deletion strains.** The gene encoding KdpA was disrupted by the insertion of a spectinomycin resistance gene into the *kdpA* gene in both the wild type and a *ktrB* disruption mutant. The transformants were grown on BG11 solid medium supplemented with spectinomycin (20 μg/ml) and buffered at pH 8.0. The disruption of *kdpA* in the transformants after segregation to homogeneity by successive streaking was confirmed by PCR amplification. In addition, the *kdpA* genes in each mutant were amplified by PCR and sequenced to confirm that the disruption was correct.

**Growth assays with *Synechocystis*.** For hyperosmotic stress assays in *Synechocystis* strains, the wild type, Δ*ktrB* mutant, Δ*kdpA* mutant, and Δ*ktrB* Δ*kdpA* double mutant were grown in BG11 medium to an $OD_{730}$ of 0.8 to 1.0 and then incubated in medium without (control) or with (osmotic shock) 3 M sorbitol for 4 h. Cells were washed with BG11 medium twice, resuspended in BG11 medium to an $OD_{730}$ of 1.0, and then spotted onto standard BG11 medium. For $K^+$ deficiency stress assays, cells were grown in BG11 medium to an $OD_{730}$ of 0.8 to 1.0. After washing the cells twice with $K^+$-depleted BG11 medium, the cells were diluted into $K^+$-depleted BG11 medium containing 5 mM KCl or without KCl to an $OD_{730}$ of 0.05, and growth was monitored.

**β-Galactosidase assays.** To study the regulation of *kdpA* expression, a 0.5-kb *kdpA* promoter sequence ($P_{kdpA}$) was fused to the bacterial β-galactosidase gene at the AflII and NdeI sites of pNS1::*lacZ*+*Cm*$^r$, and the resulting $P_{kdpA}$::*lacZ* construct was inserted into the TS1 region in the wild-type or Δ*kdpA* mutant genome using the following set of PCR primers: 5′-GGGCTTAAGATCGCCGTAGTTTACCAATG-3′ and 5′-GGGCATATGAAATTGAGATGACGAAGATGG-3′. In addition, *kdpD* (*slr1731*), *hik20* (*sll1592*, homologous to the histidine kinase domain in KdpD of *E. coli*), and *rre19* (*sll1590*, homologous to KdpE of *E. coli*) deletion strains were generated by the insertion of a kanamycin resistance cassette into these genes in the Δ*kdpA* background containing $P_{kdpA}$::*lacZ*. In order to determine whether the deletion of *hik20* affected the expression of *rre19*, the *rre19* gene was placed under the control of the constitutive *sphS* promoter (35) and inserted by homologous recombination into the TS4 region of the Δ*kdpA* Δ*hik20* strain containing $P_{kdpA}$::*lacZ*, using erythromycin resistance as a marker (+*rre19* strain). Cells resistant to erythromycin (20 μg/ml) were isolated, and the correct integration of the gene confirmed by PCR with genomic DNA. *Synechocystis* wild-type, Δ*kdpA*, Δ*kdpD*, Δ*rre19*, Δ*hik20*, and +*rre19* strains carrying the integrated $P_{kdpA}$::*lacZ* construct were assayed for β-galactosidase activity in exponentially growing cultures. Quantitative evaluation of β-galactosidase activity was carried out using permeabilized cells obtained from exponential-phase cultures incubated with a *o*-nitrophenyl-β-D-galactopyranoside substrate as previously described by Miller (36). Average (± standard deviation) activity units were calculated from three independent assays.

**Measurement of circadian rhythms of *kdpA* and *ktrB* promoter activities in *Synechocystis* cells.** The coding region of a modified firefly luciferase gene (*luc*$^+$; Promega Japan, Tokyo) was substituted for the *lacZ* sequence using the NdeI and XbaI sites in the $P_{kdpA}$::*lacZ* construct. The resultant $P_{kdpA}$::*luc*$^+$ construct was inserted into the TS1 region in the *Synechocystis* genome (37). $P_{ktrEB}$::*luc*$^+$, containing approximately 0.5 kb of the *ktrEB* promoter, was also constructed in the same manner, using 5′-GGGCTTAAGCTCAAACGGGATCAGACC-3′ and 5′-GGGCATATGGCAGATAACCAGACCGTGAA-3′. Cells were grown in BG11 liquid medium to a density of $6 \times 10^8$ to $7 \times 10^8$ cells/ml at 30°C under white fluorescent lamps (42 μmol photons $m^{-2}$ $s^{-1}$) (i.e., continuous light conditions) with shaking at 180 rpm and then diluted with BG11 medium to $2.5 \times 10^8$ cells/ml. One-hundred-eighty-microliter aliquots ($4.5 \times 10^7$ cells) of the suspension were mixed with 20 μl of 5 mM D-luciferin (Promega, Japan) dissolved in BG11 medium and transferred to 96-well microplates (Cultureplate-96; Perkin-Elmer Life Sciences Japan, Tokyo, Japan). The plates were sealed with a plate seal (Perkin-Elmer Life Sciences Japan). To reset the circadian clock of the cells, the plates were placed in the dark for 12 h at 30°C and then returned to continuous light conditions. The bioluminescence from each well was measured automatically every hour using an automated bioluminescence-monitoring apparatus (K. Onai, N. Shiraki, and M. Ishiura, unpublished data) (model CL96-4; Churitsu Electric Co., Nagoya, Japan). The data were analyzed using bioluminescence-analyzing software (Onai et al., unpublished) (SL00-01; Churitsu Electric Co., Nagoya, Japan). Circadian time (CT) was calculated by dividing the peak phase value by the period and multiplying by 24. The amplitude of the rhythm was calculated as the average ratio of peak to trough in each cycle. The period and the peak phase in each rhythm were estimated by a modified cosinor method (66).

## RESULTS

**Kdp functions as an additional $K^+$ uptake transport system.** *Synechocystis* contains two $K^+$ uptake systems, Ktr and Kdp. To elucidate the role of the *Synechocystis* Kdp transporter in $K^+$ uptake, the *kdpABGCD* operon was heterologously expressed in the $K^+$ uptake-deficient *E. coli* strain LB2003 (31). The expression of *kdpABGCD* restored $K^+$ uptake in the LB2003 strain on solid medium containing 15 and 20 mM KCl but not 10 mM KCl (Fig. 1A). The KtrABE potassium transporter of *Synechocystis* was used as a positive control. Its expression enabled growth at 10, 15, and 20 mM KCl. In liquid medium containing 12.5 mM KCl, the growth of the *kdpABGCD*-expressing strain was delayed compared with that of the *ktrABE*-expressing strain but was stimulated in comparison to the growth of the *E. coli* strain containing the empty vector (Fig. 1B). To further characterize the Kdp system, we examined the $K^+$ uptake activity of cells incubated in 200 mM HEPES-NaOH buffer in the presence of glucose. When 10 mM KCl was added, a low rate of $K^+$ uptake activity was measured in *E. coli* mutant cells expressing the *Synechocystis kdpABGCD* operon (Fig. 1C). However, much higher rates were observed in the strain expressing *ktrABE*, as reported previously (17, 18). These results indicate that the *Synechocystis* Kdp system mediates $K^+$ uptake, albeit at lower rates than Ktr.

**Ktr-driven $K^+$ uptake is required for initial cell volume recovery after hyperosmotic shock.** Since standard biochemical techniques are ineffective in monitoring changes of cell volume and ionic homeostasis in microorganisms, a direct approach was needed to assess these dynamics in single *Synechocystis* cells in order to study the membrane transport systems involved. Hence, we developed a microfluidic device that allows the fluid exchange to be performed gently and smoothly, without perturbing the cell's structural integrity. During the experiment, the cells were confined within cages surrounded by a patterned hydrogel wall (Fig. 2A to E; see also Fig. S1 in the supplemental material). The images in Fig. 2D and E show that the water-permeable hydrogel wall used to trap the cells in the slots allowed replacement of the liquid without influencing the cells mechanically. To determine the requirement of $K^+$ for cell recovery after hyperosmotic shock, wild-type *Synechocystis* cells were incubated in the microfluidic device either in standard BG11 medium or potassium-depleted (K0) medium (0.1 osmol) and then subjected to hyperosmotic shock by the addition of 3 M sorbitol (3.6 osmol) to the respective medium (Fig. 2F and G). In standard BG11 medium, the cell volume rapidly decreased by 54.8% at 120 s after hyperosmotic shock (Fig. 2F and G). The subsequent cell volume recovery occurred in a biphasic response. During the first recovery phase, from 120 s to 300 s, the cell volume increased by 12.2%, and during the second recovery phase, from 300 s to 3,600 s, it recovered by 13.4%. When the same experiment was performed with cells in potassium-free

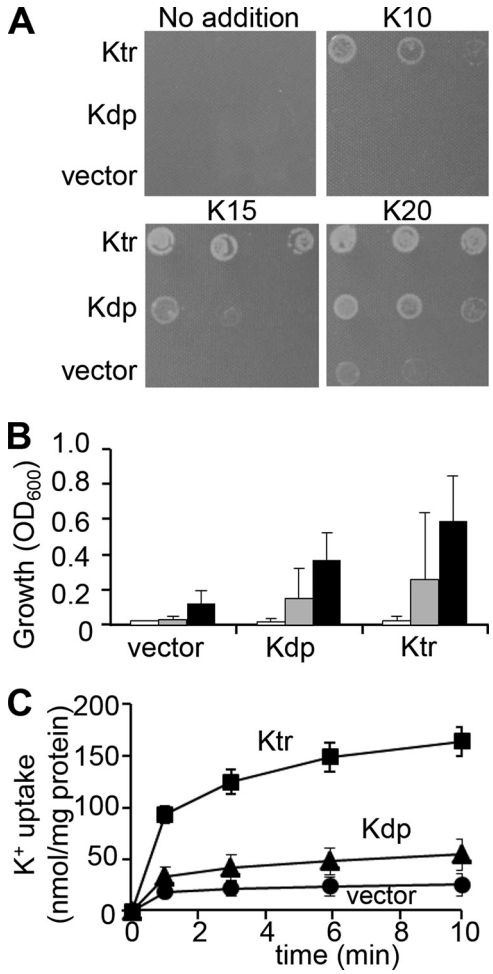


**FIG 1** *Synechocystis* Kdp-mediated $K^+$ uptake plays a minor role compared to that of Ktr. (A) Complementation of the $K^+$ uptake-deficient *E. coli* strain LB2003 by *Synechocystis kdpABGCD*. LB2003 cells containing *kdpABGCD*, *ktrABE* (as a positive control) (18), or the empty vector were grown on solid synthetic medium supplemented without added KCl or with 10 mM, 15 mM, or 20 mM KCl. The first spot in each row represents an $OD_{600}$ of 0.005, which is diluted 1:10 for each spot thereafter. (B) Growth of *E. coli* LB2003 containing empty vector, *kdpABGCD*, or *ktrABE* in liquid synthetic medium with 12.5 mM KCl at 5 h (open bars), 21.5 h (gray bars), and 25.5 h (black bars). The values are the means and standard deviations (SD) of the respective results ($n = 3$ for empty vector, $n = 10$ for *kdpABGCD*, and $n = 4$ for *ktrABE*). (C) $K^+$ uptake activities by *E. coli* LB2003 containing KdpABGCD, KtrABE, or the empty vector. $K^+$-depleted cells were energized with glucose, and at time zero, 10 mM KCl was added to the medium. The KtrABE expression vector and the empty vector were the same constructs as reported previously (18). Samples were taken at the times indicated in the figure. Error bars denote the SD of the results from four independent experiments.

K0 medium (which contained $Na^+$ instead of $K^+$ in the BG11 medium), the same rapid initial decrease of cell volume was recorded within 120 s. However, no cell volume recovery was observed from 120 s to 300 s. The cell volume even seemed to decrease slightly more, by 2.8%, at 300 s (Fig. 2G and Table 1). While the first recovery phase was absent in K0 medium, a relatively quick recovery of cell volume started at 600 s (Fig. 2G and Table 1). These results show that cell volume recovery after hyperosmotic stress was biphasic and depended on $K^+$ uptake by the *Synechocystis* cells.

**Ktr contributes more to high-osmolarity acclimation than Kdp does in *Synechocystis*.** To distinguish which transporter is responsible for the $K^+$ uptake that ensures rapid volume recovery after hyperosmotic stress of *Synechocystis* cells, mutants defective in the two $K^+$ transport systems were analyzed. In addition to the previously described Δ*ktrB* mutant (17, 18), we generated a Δ*kdpA* mutant, which is defective in the *kdpA* gene that encodes the permease subunit of Kdp. *Synechocystis* KdpA shares 59% identity with *E. coli* KdpA. In addition, a Δ*ktrB* Δ*kdpA* double mutant was generated. In a first experiment, the survival of these cells under conditions of harsh osmotic shocks was investigated. After their incubation in liquid medium containing 3 M sorbitol for 4 h, cells were spotted onto plates containing solid BG11 medium without sorbitol (Fig. 3A). The treatment strongly decreased the growth of both Ktr mutants, the Δ*ktrB* strain and the Δ*ktrB* Δ*kdpA* strain, while the wild type grew well. The Δ*kdpA* strain grew better than the other two mutants but not as well as the wild type (Fig. 3A).

In a second experiment, the microfluidic device was used to evaluate changes in cell volume in response to hyperosmotic stress in BG11 medium containing sufficient amounts of $K^+$ (Fig. 3B). The cell volumes of the Δ*ktrB* strain, the Δ*kdpA* strain, and the Δ*ktrB* Δ*kdpA* strain had shrunk to 40.9 to 48.4% after 120 s, similar to the shrinkage of the wild type (Fig. 2G and 3C and Table 2). Cells of the wild type began to swell again during the first phase of recovery (120 to 300 s). In contrast, the cell volume of the Δ*ktrB* Δ*kdpA* mutant remained small in the first phase of recovery (35.0 to 40.9%) and started to increase to 66.1% only much later, at 3,600 s. Using the two single mutants, the individual contributions of Ktr and Kdp to the cell volume changes could be estimated (Fig. 3C and Table 2). The Δ*ktrB* cells, like those of the double mutant, continued to shrink during the time span when the wild type showed its first recovery phase (120 to 300 s). Then, after 600 s, the volume of the Δ*ktrB* cells increased, eventually reaching a size similar to the volume of the wild type at 3,600 s (Fig. 3C). The Δ*kdpA* cells recovered faster than the Δ*ktrB* cells but less rapidly than the wild-type cells; recovery toward the original volume initiated within 180 to 300 s. Based on these results, we conclude that Ktr represents the major contributor to $K^+$ uptake for initial cell volume recovery from hyperosmotic stress, while Kdp was likely not involved or was involved only to a very small extent.

**KdpA functions as an uptake system at trace $K^+$ amounts in *Synechocystis*.** To further elucidate the function of Kdp in *Synechocystis*, we compared the growth of the wild type, the Δ*ktrB* strain, and the Δ*ktrB* Δ*kdpA* double mutant in $K^+$-limited medium (Fig. 4). The growth of all the strains was comparable in the medium supplemented with 5 mM $K^+$ (Fig. 4B). However, in $K^+$-depleted medium containing just trace amounts of $K^+$, the Kdp-expressing cells (the wild type and Δ*ktrB* strain) grew better than the Δ*kdpA* strain (Fig. 4A). These results suggest that Kdp mediated $K^+$ uptake at very low $K^+$ concentrations.

Hence, the expression of *kdpA* under various abiotic stress conditions, including $K^+$ deficiency, was determined by a reporter gene approach. To this end, we generated *Synechocystis* cells expressing the *lacZ* gene under the control of the *kdpA* promoter (0.5 kb long). The reporter constructs were integrated into the neutral TS1 regions, both in wild-type and Δ*kdpA* backgrounds. In the wild-type background, the expression of the *kdpA* promoter construct was enhanced approximately 3.1-fold after 24 h under conditions of $K^+$ deficiency (Fig. 5A and B). Under the same con-

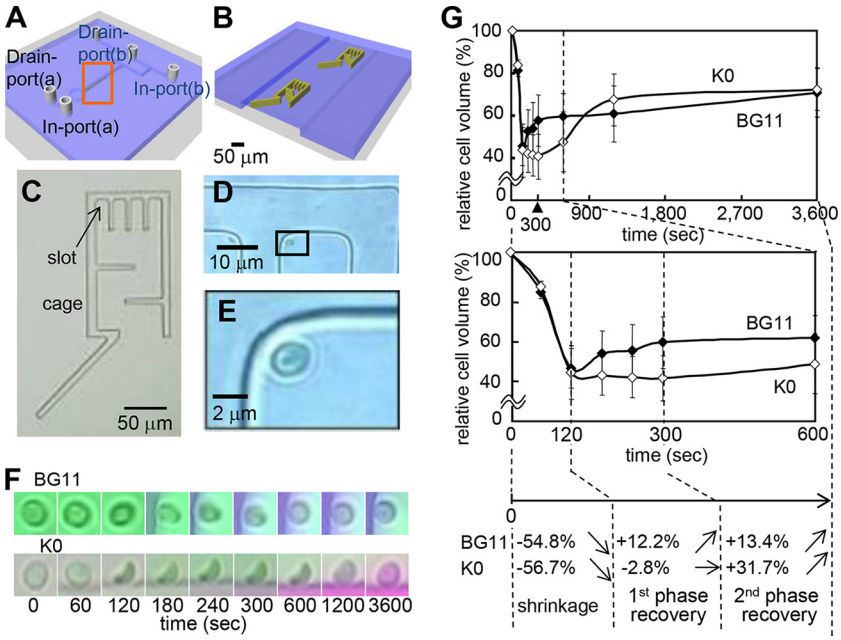


**FIG 2** $K^+$-dependent dynamic changes in the volumes of wild-type cells subjected to hyperosmotic stress. (A to E) Microfluidic device for on-chip continuous monitoring of individual cells of *Synechocystis* sp. PCC 6803. (A and B) Ten cages at a time were placed in the microfluid channel. Panel B is an enlargement of the boxed area in panel A, showing two of the cages. (C) Photograph of a cage surrounded by the hydrogel wall. The arrow is pointing at one of the slots that hold the cells during the measurements. (D and E) Images of a *Synechocystis* cell inside a slot. Panel E is an enlargement of the boxed area in panel D. (F and G) $K^+$ uptake is required for the recovery of cell volume during hyperosmotic stress. Wild-type cells inside the microfluidic device were incubated either in standard BG11 medium or in $K^+$-depleted K0 medium (K0) and then (corresponding to time zero) subjected to hyperosmotic shock by the addition of 3 M sorbitol (in the same medium). (F) Images of single cells recorded over time during the hyperosmolarity treatment. (G) Changes in volume of *Synechocystis* wild-type cells in standard BG11 medium or K0 medium over time, calculated from data recorded by the device. The different phases, indicated by broken lines, are as follows: cell shrinkage after the hyperosmotic shock, first phase of recovery (120 to 300 s), and second phase of recovery (300 to 3,600 s). The cell volume was calculated from the cell diameter using Image J as described in Materials and Methods. The relative cell volume at time zero was set at 100% in each case. Error bars denote the SD of the results from at least 7 cells. The percentages in panel G correspond to the data obtained in standard BG11 medium for the different phases following hyperosmotic shock (Table 1). Biphasic cell volume changes of *Synechocystis* during hyperosmotic stress are shown. Transfer of cells from isotonic to hyperosmotic medium triggered efflux of water from the cells, resulting in reduction of cell volume. This quick adaptation occurred in the first phase of the cell recovery response in the $K^+$-containing medium (BG11) but not in $K^+$-depleted medium (K0). During the second phase of cell adaptation, compatible solute biosynthesis and accumulation may have occurred, which induced more water influx and cell volume recovery (4, 5). Arrows indicate the trends of changes in volume.

ditions, more than 2 times higher expression (approximately 7.9-fold) of the *kdpA* promoter was measured in the Δ*kdpA* strain. This result suggested that the decreased intracellular $K^+$ level due to the lack of KdpA-mediated $K^+$ uptake activity in the Δ*kdpA* background led to enhanced induction of the *kdpA* promoter. In contrast, the *kdpA* promoter showed only small responses to either salinity stress or hyperosmotic shock in the wild-type and Δ*kdpA* backgrounds (Fig. 5C and D).

**Distinct regulation of *kdp* expression in *Synechocystis*.** The arrangement of the *kdp* operon in *Synechocystis* differs from the situation in *E. coli*, where the expression of the *kdp* operon is mediated by a two-component system comprising the sensor kinase KdpD and the response regulator KdpE (Fig. 6A) (28). An additional gene, *kdpG*, is situated between *kdpB* and *kdpC* in *Synechocystis*. The genes encoding the corresponding two-component system are also arranged differently than in *E. coli*. The *Synechocystis* KdpD homolog is divided into two separate proteins. The annotated KdpD in the *kdpABGCD* operon (CyanoBase; http://genome.microbedb.jp/cyanobase/Synechocystis/genes/slr1731) corresponds only to the N-terminal region of the canonical histidine kinase. Another *Synechocystis* gene, annotated as histidine kinase 20 (Hik20), corresponds to the C-terminal region of KdpD

**TABLE 1** Contribution of extracellular $K^+$ to recovery of cell volume in wild-type *Synechocystis* cells after hyperosmotic shock

| Medium | Cell volume at time zero (%) | % of cell volume recovered at indicated time (s)[a] | | | | | | | |
|---|---|---|---|---|---|---|---|---|---|
| | | 60 | 120 | 180 | 240 | 300 | 600 | 1,200 | 3,600 |
| BG11 | 100 | 81.0 | 45.2 | 52.4 | 53.6 | 57.4 | 57.4 | 60.5 | 70.8 |
| K0 | 100 | 83.7 | 43.3 | 41.8[b] | 41.0[b] | 40.5[c] | 47.3 | 67.2 | 72.2 |

[a] Osmotic shock was induced with 3 M sorbitol. The percentage of the cell volume at each time point compared to the volume at 0 s (set at 100%) is shown. The smallest cell volume for each condition is underlined. Values are summaries of the results shown in Fig. 2G. Standard deviations (SD), based on the results for at least 7 cells, are shown in Fig. 2G.

[b] $P < 0.05$ versus the results for the wild type in BG11 medium.

[c] $P < 0.01$ versus the results for the wild type in BG11 medium.

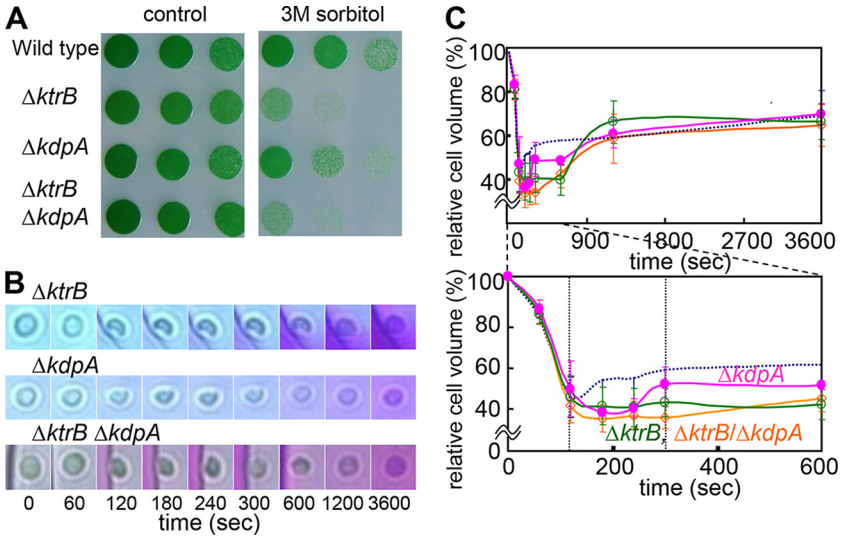


**FIG 3** Effects of disruption of *ktrB* and *kdpA* on the hyperosmotic stress response in *Synechocystis* cells. (A) Growth of *Synechocystis* wild type, Δ*ktrB* mutant, Δ*kdpA* mutant, and Δ*ktrB* Δ*kdpA* double mutant spotted onto standard BG11 medium with 1:5 serial dilutions from an $OD_{730}$ of 1 after incubation in medium containing 3 M sorbitol for 0 h (left) or 4 h (right). (B) Representative time courses of single cells (Δ*ktrB* mutant, Δ*kdpA* mutant, and Δ*ktrB* Δ*kdpA* double mutant) inside the microfluidic device showing shrinkage and recovery after being subjected to hyperosmotic stress by replacement of the standard BG11 medium with the medium containing 3 M sorbitol at 0 s. (C) Profiles of volume changes of cells of the Δ*ktrB* mutant (green), Δ*kdpA* mutant (pink), and Δ*ktrB* Δ*kdpA* double mutant (orange) determined from the microscopy images taken by the camera attached to the microfluidic device. The bottom panel shows a subset of the data in the top panel (0 to 600 s). The dotted lines correspond to the volume changes of the wild type; the data are the same as are shown in Fig. 2G. Error bars denote SD of the results from 5 to 8 cells (Table 2).

in *E. coli*. The *hik20* gene forms a putative operon with the gene for the response regulator homolog KdpE, named *rre19* in *Synechocystis*. The *hik20-rre19* gene operon, encoding truncated KdpD-like and KdpE proteins, is situated in reverse orientation upstream from the *kdpA* gene (Fig. 6A). To study the regulation of *kdp* gene expression in *Synechocystis*, we deleted *kdpD*, *hik20*, or *rre19* in the Δ*kdpA* strain containing the reporter construct $P_{kdpA}$::*lacZ*. The Δ*kdpA* strain was chosen as the parental strain because it showed the most sensitive reaction to low concentrations of $K^+$ (Fig. 5B and 6B). Disruption of *kdpD* had only a small effect on the *kdpA* promoter activity compared with its activity in the parental strain. However, the deletion of either *hik20* or *rre19* completely prevented the induction of the *kdpA* promoter-driven reporter gene (Fig. 6B). Since the *rre19* gene is located downstream from *hik20* (Fig. 6A), we tested whether the observed effect of the *hik20* deletion was indirectly caused by polar effects disrupting *rre19* expression and not by the deletion of *hik20* itself. Thus, a Δ*hik20* mutant was generated that constitutively expressed *rre19* under the control of the *sphS* promoter (35). The constitutive expression of *rre19* in the Δ*hik20* strain did not restore the activity of the *kdpA* promoter at low $K^+$ concentrations. Collectively, these results strongly suggested that the expression of the *kdp* operon was positively regulated by both Hik20 and Rre19 but not by KdpD.

**The *kdp* and *ktr* genes show circadian expression in *Synechocystis*.** Photoautotrophic organisms are exposed to daily periodic changes of light in their natural environment, and $K^+$ homeostasis is controlled by the circadian oscillation of $K^+$ transport in various species, including plant cells (38–40). *Synechocystis* may also be faced with periodic requirements of $K^+$, which is taken up by Kdp and Ktr in environments containing small amounts of $K^+$. The database on circadian oscillation in *Synechocystis* did not show apparent rhythms of the expression of the genes encoding subunits of Kdp and Ktr, namely, KdpA and KtrB (37) (KEGG Expression Database; http://www.genome.jp/kegg/expression/). The circadian oscillation of *kdp* and *ktr* expression in *Synechocystis* was tested using a real-time bioluminescence-monitoring system.

**TABLE 2** Changes in cell volume of the $K^+$ transporter mutants after hyperosmotic shock

| Strain | Cell volume at time zero (%) | % of cell volume recovered at indicated time (s)[a] | | | | | | | |
|---|---|---|---|---|---|---|---|---|---|
| | | 60 | 120 | 180 | 240 | 300 | 600 | 1,200 | 3,600 |
| Wild type[b] | 100 | 81.0 | 45.2 | 52.4 | 53.6 | 57.4 | 57.4 | 60.5 | 70.8 |
| Δ*ktrB* mutant[c] | 100 | 82.7 | 44.4 | 40.7[e] | 40.1[d] | 42.2[e] | 41.4[e] | 67.8 | 68.0 |
| Δ*kdpA* mutant | 100 | 85.1 | 48.4 | 37.8[e] | 39.7[d] | 50.7 | 50.1 | 62.3 | 71.4 |
| Δ*ktrB* Δ*kdpA* mutant | 100 | 82.8 | 40.9 | 35.0[e] | 36.4[e] | 35.5[e] | 44.0[e] | 60.3 | 66.1 |

[a] Osmotic shock was induced with 3 M sorbitol. The percentage of the cell volume compared to the volume at 0 s (set at 100%) is shown, and the smallest cell volume for each condition is underlined. Values are summaries of the results shown in Fig. 3C.
[b] The wild type data are shown as a control and are the same data shown in Table 1.
[c] SD for all mutant strains, based on the results for 5 to 8 cells, are shown in Fig. 3C.
[d] $P < 0.05$ versus the results for the wild type.
[e] $P < 0.01$ versus the results for the wild type.

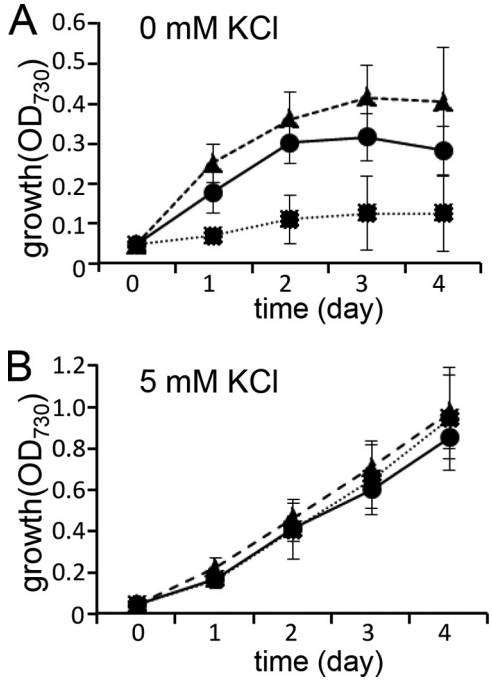


**FIG 4** Significance of Kdp-mediated $K^+$ uptake in $K^+$-depleted medium. *Synechocystis* wild type (circles), Δ*ktrB* mutant (triangles), and Δ*ktrB* Δ*kdpA* double mutant (squares) were grown in $K^+$-depleted medium without KCl (A) or with 5 mM KCl (B). Error bars denote SD of the results from six independent experiments.

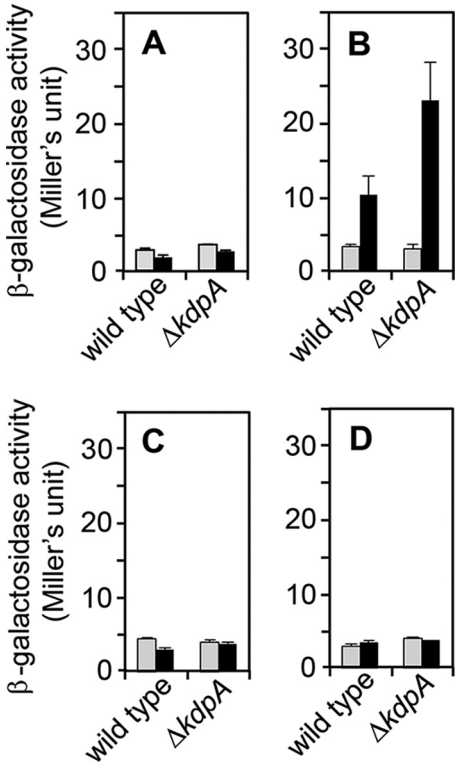


**FIG 5** Induction of the *kdp* operon by abiotic stress. *Synechocystis* wild type and the Δ*kdpA* mutant carrying the $P_{kdpA}$::*lacZ* reporter construct in their genomes were grown in BG11 medium to an $OD_{730}$ of 0.6 to 2.0. β-Galactosidase activity was measured at the beginning of the assay (0 h, gray bars) or after 24 h of incubation (black bars) of the cells in BG11 medium (i.e., no stress) (A), $K^+$-depleted medium (B), BG11 medium containing 500 mM NaCl (salt stress) (C), or medium containing 400 mM sorbitol (osmotic stress) (D).

Cells expressing firefly luciferase driven by the circadian-controlled promoter of *dnaK*, a gene encoding a heat shock protein, were used as controls (Fig. 7A, top) (41). The expression of *kdpA* exhibited circadian oscillation with a period (wavelength of the cosine curve) of 23.0 ± 0.2 h, close to the period of *dnaK* expression (22.8 ± 0.4 h). The expression of *kdpA* reached its highest level at the circadian time of 23.7 ± 0.5 h, corresponding to subjective dawn (Fig. 7A and Table 3). The genes *ktrE* and *ktrB* share the same cistron due to overlapping of the stop codon of *ktrE* and the initiation codon of *ktrB* (18, 42). The expression of *ktrEB* showed a circadian rhythm with the peak at 23.0 ± 0.5 h, almost consistent with that of *kdpA* (Table 3).

## DISCUSSION

Although $K^+$ uptake transporters overall contribute to maintaining $K^+$ as the major cation in the cell, each type of $K^+$ transporter is likely to have a divergent individual physiological role. *Synechocystis* contains two of the three classes of $K^+$ uptake systems found in *E. coli*, the well-characterized Ktr (18, 28, 33, 34, 43) and the less-characterized Kdp (17). Despite many efforts in analyzing Kdp in *Anabaena* strains (28), *E. coli* (21–25), and *Staphylococcus aureus* (19, 27), its function in the important model cyanobacterium *Synechocystis* is only scarcely known due to the existence of a Ktr-type $K^+$ uptake system and the absence of specific mutants (17, 18). Preliminary investigations with *Synechocystis* mutants bearing defects in *ktr* or *kdp* genes indicated a major role of Ktr for $K^+$ uptake in salt-shocked *Synechocystis* cells (17). This finding could indicate that the *kdp* genes encode an inactive transporter in *Synechocystis*. Hence, we first aimed to prove the potential role of the *Synechocystis* Kdp in $K^+$ transport by complementing a $K^+$ uptake mutant of *E. coli*. These experiments showed that the expression of cyanobacterial Kdp allowed the growth of the $K^+$ uptake-deficient *E. coli* (Fig. 1A and B). However, even in the *E. coli* system, the Ktr-mediated activity was dominant because the promotion of growth and, particularly, the $K^+$ uptake activity were much higher in *ktrABE*-expressing cells than in the cells expressing *kdpABGCD* (Fig. 1C). Nevertheless, these experiments clearly revealed that the *Synechocystis kdp* operon encodes an active $K^+$ transporter.

To identify the role of the different $K^+$ transport systems, we first aimed to study the cellular response to sudden shocks of high osmolarity, since the osmostress acclimation involves dramatic changes in $K^+$ fluxes (5). The conventional experimental approaches used to elucidate the physiological responses of cells to abiotic and biotic stress commonly make use of large populations of cells that are transferred from one medium into another. The data obtained from those experiments are therefore the averages of many individual responses from many different cells, some of which may not actually undergo osmoacclimation. In contrast, microfluidic devices make it possible to characterize and monitor cellular responses in individual living cells in real time. To realize a single-cell analytical approach on a microfluidic platform with real-time monitoring, physical stress on the cells caused by the fluid exchange must be minimized. Approaches using lab-on-a-chip devices enable the monitoring and manipulation of nanopar-

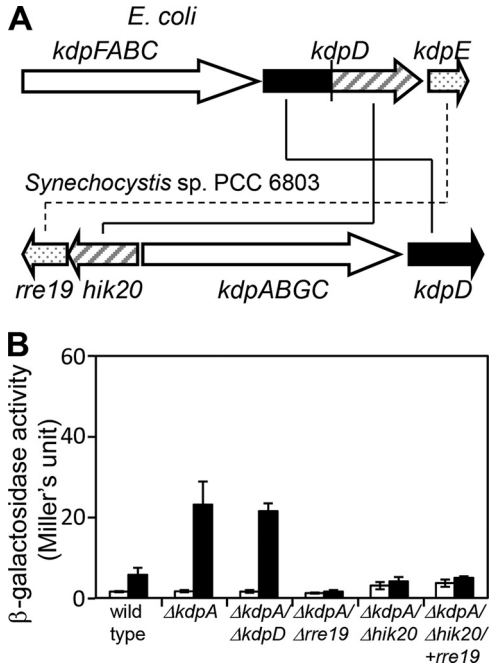


**FIG 6** Regulation of *kdp* operon expression by histidine kinase and response regulator. (A) Comparison of the gene arrangements of the *E. coli* and *Synechocystis kdp* operons. Homologous genes are denoted by the same color or pattern. (B) β-Galactosidase activity was measured in exponentially growing *Synechocystis* wild type or various mutant strains carrying $P_{kdpA}$::*lacZ* before (open bars) or after (black bars) incubation in $K^+$-depleted medium for 24 h. The deletions present in the strains tested are indicated under the bars. +*rre19* denotes the reintroduction of *rre19* under the control of a constitutive promoter into the Δ*kdpA* Δ*hik20* background to control for a possible effect of the deletion of *hik20* on *rre19* expression. Results are means ± standard errors of the results from three experiments.

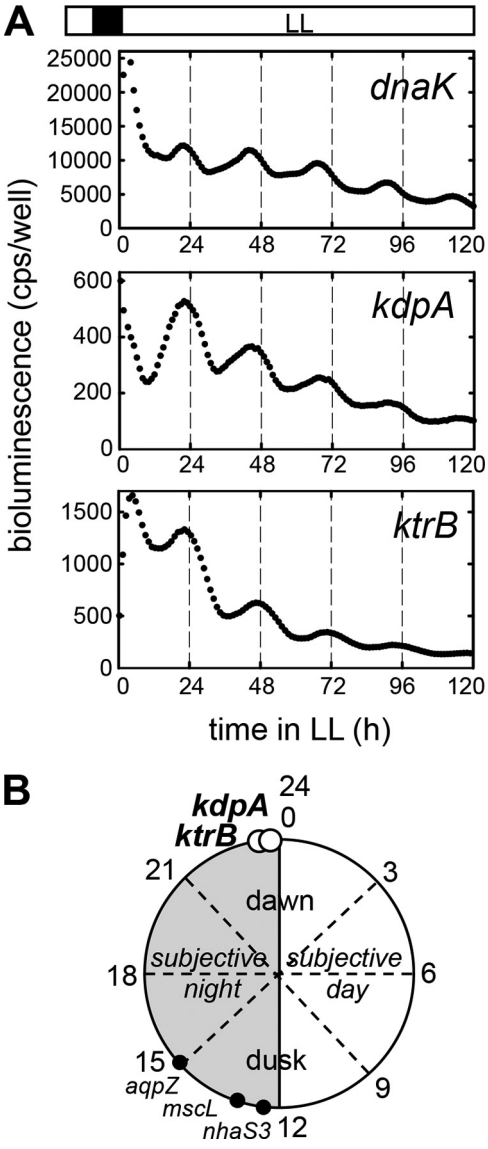


**FIG 7** Circadian rhythm of *kdpA* expression in *Synechocystis*. (A) Representative circadian oscillation profiles of bioluminescence measurements from *Synechocystis* strains containing $P_{dnaK}$::$luc^+$, $P_{kdpA}$::$luc^+$, and $P_{ktrEB}$::$luc^+$ are shown. The cell cultures were preincubated in the dark for 12 h (filled square) and then transferred to continuous light conditions (LL; open rectangle). Essentially the same profiles were obtained from three independent experiments. Detailed values are listed in Table 3. (B) Model of the circadian rhythm of *kdpA* and *ktrB* expression in *Synechocystis*. The expression peaks of the genes encoding the membranous transport proteins *kdpA* and *ktrB* are marked by open circles at the corresponding circadian times. The previously reported peaks of *aqpZ* (aquaporin) (57), *nhaS3* ($Na^+/H^+$ antiporter) (56), and *mscL* (mechanosensitive channel large conductance) (58) are also indicated (filled circles).

ticles and biomolecules (44). The design of the device and the materials used in its construction are of critical importance for successful monitoring of individual cells over extended periods of time. There have been reports of cages made of permeable membranes (45). Although a monitoring device for animal cell cultures has been reported (46–48), it was not applicable to microorganisms like *Synechocystis* due to its smaller size of 2 to 4 μm in diameter. The size of the cells being analyzed is a critical aspect, since the physical force exerted by the flow of the medium can affect the cells in the course of observing cell volume changes. Therefore, we developed a new microfluidic device and used it to confirm that individual *Synechocystis* cells required $K^+$ to protect themselves against hyperosmotic shock (Fig. 2).

The data in Table 1 and in Fig. 2G illustrate how water and $K^+$ flux accompanied volume changes of single cells under hyperosmotic stress conditions. As a first response to the stress, water flowed out of the cells, resulting in cell shrinkage (54.8% decrease at 120 s). $K^+$ ions in the liquid medium were taken up to ensure fast recovery of volume (Fig. 2G). This rapid $K^+$ uptake was mainly driven via the Ktr transport system when the medium contained sufficient concentrations of $K^+$ (Fig. 3C and Table 2). This finding was consistent with the idea that Ktr functions as a $K^+$ uptake system during hyperosmotic stress in *Synechocystis* (18). This conclusion is based on the following two findings: (i) the wild-type cells lacked the first phase of recovery (120 to 300 s) in a $K^+$-depleted medium (Fig. 2G and Table 1) and (ii) the cells defective in Ktr, i.e., the Δ*ktrB* and Δ*ktrB* Δ*kdpA* mutants, also lacked the first recovery phase even under conditions of sufficient $K^+$ (Fig. 3C and Table 2), whereas the Δ*kdp* mutant behaved like the wild type under these conditions. In the second phase of cell volume recovery, the cell volume of the wild type increased very slowly by a moderate 13.4% only at 3,600 s in BG11 medium (Fig. 2G and Table 1). The full recovery of volume probably needs the synthesis and accumulation of the compatible solute glucosylglycerol in the second or later phase of osmoacclimation, which in-

**TABLE 3** Circadian expression of *kdp and ktr*[a]

| Construct expressed | Period | Peak phase (h) | Circadian time of peak phase | Amplitude | No. of wells analyzed |
|---|---|---|---|---|---|
| $P_{dnaK}$::*luc*$^+$ | 22.8 ± 0.4 | 21.4 ± 0.6 | 22.5 ± 0.6 | 1.40 ± 0.03 | 11 |
| $P_{kdpA}$::*luc*$^+$ | 23.0 ± 0.2 | 22.6 ± 0.5 | 23.7 ± 0.5 | 1.70 ± 0.03 | 7 |
| $P_{ktrEB}$::*luc*$^+$ | 22.5 ± 0.7 | 21.6 ± 0.5 | 23.0 ± 0.5 | 1.18 ± 0.10 | 6 |

[a] Values (means ± SD) are summaries of the results shown in Fig. 7.

duced more water influx and recovery of cell volume (4, 5). During the second phase of cell adaptation, not only the biosynthesis and accumulation of the compatible solute but also an influx of sorbitol into the cells may have occurred. Sorbitol influx has been shown to occur in cells of wild-type *Synechocystis* and a mutant unable to synthesize the compatible solute glucosylglycerol when they were treated with large amounts of external sorbitol (49). Taken together, these results suggest that the uptake of $K^+$ into the cells via $K^+$ transporters was required for the first phase of recovery and that Ktr especially but not Kdp contributed significantly to this first recovery phase.

The values for cell volume are presented as relative cell volume determined by conversion of each area of the light microscopy images (Fig. 2 and 3 and Tables 1 and 2). The results for the oval cells, which are not isotropically shaped, might bear errors to some extent. Moreover, it is possible that during these experiments, the plasma membrane separated from the cell wall, similar to plasmolysis seen in plant cells, which may somehow decrease the total extent of cell shrinkage (50). Under the experimental conditions used here, we cannot rule out these possible influences on the exact measurement of the relative cell volumes.

To reveal a physiological function separate from osmoacclimation of Kdp in *Synechocystis*, we compared the growth rates of the wild type, the Δ*ktrB* mutant, and the Δ*kdpA* Δ*ktrB* double mutant at different levels of external $K^+$ (Fig. 4). The results of these experiments illustrated the physiological importance of Kdp at trace concentrations of $K^+$. The specific role of Kdp at trace $K^+$ amounts is indirectly supported by the notion that the expression of *kdp* by cells exposed to a low concentration (μmol) of $K^+$ in our reporter gene experiments with *Synechocystis* was induced similarly to previously reported results in *Anabaena* (51) and *Staphylococcus aureus* (19, 21). The presence of two transport systems, Ktr and Kdp, with different affinities for $K^+$ may contribute to an increase in the survival rate of *Synechocystis* and lead to an expansion of its habitat.

Next, we investigated the regulation of the expression of the *Synechocystis kdp* operon. It showed a clear response to $K^+$-limited conditions that was analogous to the situation in many other microorganisms (Fig. 5B) (28). In *E. coli*, the addition of either ionic or nonionic impermeable solutes also induced *kdp* operon expression (52). However, the *Anabaena* L-31 *kdp2* operon did not respond to increases in osmolarity imposed by saline stress (28, 53). Similarly, the *Synechocystis kdp* operon was not induced by salt or osmotic stress (Fig. 5C and D). Sensing of the extracellular $K^+$ concentration is critical for the regulation of *Synechocystis* and *Anabaena kdp* expression but not osmotic stress. In *E. coli*, the stress- and $K^+$-dependent upregulation of *kdp* depends on the two-component system encoded by *kdpDE* (24, 26). Similarly, *kdpA* was induced by 2 M NaCl in *Staphylococcus aureus* (19). In the latter bacterium, the high-salt-inducible Kdp and the constitutively expressed Ktr participated cooperatively in the alleviation of salt and osmotic challenges. In *Synechocystis*, Kdp showed a smaller contribution to high-osmolality acclimation, at least under our study conditions (Fig. 3 and 5). The *Synechocystis kdp* operon has a unique organization that is different from that of the *E. coli* and *Staphylococcus aureus kdp* operons (Fig. 6A) (28). In particular, the histidine kinase KdpD of *E. coli* is divided into two parts, as was reported before for the homologous operon in *Anabaena* L-31 (28). Deletion of either *hik20* or *kdpD* revealed that Hik20 but not KdpD was required for sensing low extracellular $K^+$ concentrations and the induction of the *kdpABGCD* operon under these conditions (Fig. 6B). The function of the truncated KdpD in *Synechocystis* remains unclear. In *E. coli*, the N-terminal domain of KdpD, corresponding to the *Synechocystis* KdpD, was shown to be involved in modulating the activity of the Kdp transport system *in vivo* and *in vitro* by enhancing *kdp* expression (28). Moreover, the functionality of the truncated KdpD form of *Anabaena* sp. L-31 fused to the C-terminal domain of the *E. coli* KdpD has been shown. The resulting *Anabaena-E. coli* chimeric KdpD was able to complement an *E. coli kdpD* mutation in regard to sensing $K^+$ deficiency (54). Moreover, the recombinant KdpE of *Anabaena* sp. L-31, which is highly similar to Rre19, was able to bind in a phosphorylation-dependent manner to the promoter of the *Anabaena kdp2* operon. Thus, the cyanobacterial two-component system, which is encoded by *hik20* and *rre19* in *Synechocystis*, is responsible for the $K^+$-dependent expression of the *kdpABGCD* operon. Possibly the missing N-terminal part of the *E. coli* KdpD in Hik20 is responsible for the lack of induction of the system by hyperosmotic stress, in contrast to *E. coli* (28). However, the *kdp* operon encoding the structural proteins is induced by desiccation stress in *Anabaena* strains (53, 55). Further studies are still needed to clarify the physiological role of the two-component system of Kdp.

In their natural environment, microorganisms regularly have to cope not only with changing salinities but also with a scarcity of essential elements, such as $K^+$. The circadian oscillation of *kdp* and *ktr* expression found in this study suggests an involvement of Kdp and Ktr in the regulation of diurnal potassium homeostasis in *Synechocystis* (Table 3 and Fig. 7). Despite the apparent difference in function between Kdp and Ktr, their peaks of circadian oscillations were consistent with each other but occurred at different times than those of other membrane transport proteins involved in acclimation to environmental changes (56–58) (Fig. 7B). By increasing *kdp and ktr* expression and, possibly, $K^+$ uptake at the beginning of the light period, cells may prepare themselves for the acquisition of $K^+$ required to support processes of the regular diurnal metabolism, such as photosynthesis, respiration, and/or cell division (59). Consequently, the circadian rhythms of the $K^+$ uptake activities mediated by the two transporters may have evolved in order to meet $K^+$ requirements that fluctuate with daily

rhythmic changes. Such changes in cellular $K^+$ transport have been shown for eukaryotic algae. *Gonyaulax*, a unicellular marine photosynthetic dinoflagellate, exhibited a 2-fold increase of $K^+$ content in its cells at the end of the light period compared with the level at the beginning (60), whereas light-stimulated $K^+$ uptake played a crucial role for growth in the red alga *Porphyra leucosticte* (61). This alga showed daily cycles of $K^+$ enrichment and subsequent turgor-driven enlargement that were disturbed by $K^+$ limitation or inhibitors of $K^+$ transport. In plants, the $K^+$ concentration in the guard cells starts to increase in the morning, reaching the highest level at dusk (62). In the motor cells of the tropical tree species *Samanea saman*, the expression of $K^+$ channels oscillated rhythmically during light-dark cycles (63). It can be argued that the circadian control system of cells must be able not only to respond to environmental changes but also to prepare for such conditions in advance (64). Phototrophic organisms like *Synechocystis* therefore induce the synthesis of their $K^+$ uptake system at dawn, in order to prepare themselves for the control of turgor pressure and membrane potential in their cells for diurnal activities.

Collectively, our study clearly revealed that each type of $K^+$ transporter is likely to have an individual physiological role. We demonstrated that, compared with Kdp-mediated activity, Ktr-mediated $K^+$ uptake activity is dominant under high-osmolarity conditions in the presence of relatively high external $K^+$. However, $K^+$ deficiency frequently occurs in the natural environment of cyanobacteria, which have been found in harsh habitats (65). Under such conditions, Kdp will become the main transporter supplying $K^+$ to the cells, while Ktr only plays a minor role. This scenario suggests that Kdp may function to keep the intracellular $K^+$ concentration above the basal level. The two *Synechocystis* $K^+$ uptake systems, Ktr and Kdp, therefore fulfill distinct, unique roles that help to contribute to the survival of these cyanobacteria living in a variable, stressful, light-dark cycle environment.

## ACKNOWLEDGMENTS

We thank Ryo Iitsuka, Hideyuki Matsumoto, and Naomi Hoshi (Tohoku University) for technical assistance, Gerald Kada and W. Travis Johnson (Agilent Technologies) for comments on the manuscript, and Anke Reinders (University of Minnesota) for critical reading of the manuscript.

This work was supported by the Japan Society for the Promotion of Science (grants 24246045, 24580100, 24658090, and 25292055).

## REFERENCES

1. **Whatmore AM, Chudek JA, Reed RH.** 1990. The effects of osmotic upshock on the intracellular solute pools of *Bacillus subtilis*. J Gen Microbiol **136:**2527–2535. http://dx.doi.org/10.1099/00221287-136-12-2527.
2. **Whatmore AM, Reed RH.** 1990. Determination of turgor pressure in *Bacillus subtilis*: a possible role for $K^+$ in turgor regulation. J Gen Microbiol **136:**2521–2526. http://dx.doi.org/10.1099/00221287-136-12-2521.
3. **Record MT, Jr, Courtenay ES, Cayley S, Guttman HJ.** 1998. Biophysical compensation mechanisms buffering *E. coli* protein-nucleic acid interactions against changing environments. Trends Biochem Sci **23:**190–194. http://dx.doi.org/10.1016/S0968-0004(98)01207-9.
4. **Dinnbier U, Limpinsel E, Schmid R, Bakker EP.** 1988. Transient accumulation of potassium glutamate and its replacement by trehalose during adaptation of growing cells of *Escherichia coli* K-12 to elevated sodium chloride concentrations. Arch Microbiol **150:**348–357. http://dx.doi.org/10.1007/BF00408306.
5. **Hagemann M.** 2011. Molecular biology of cyanobacterial salt acclimation. FEMS Microbiol Rev **35:**87–123. http://dx.doi.org/10.1111/j.1574-6976.2010.00234.x.
6. **Los DA, Murata N.** 1999. Responses to cold shock in cyanobacteria. J Mol Microbiol Biotechnol **1:**221–230.
7. **Buurman ET, Kim KT, Epstein W.** 1995. Genetic evidence for two sequentially occupied $K^+$ binding sites in the Kdp transport ATPase. J Biol Chem **270:**6678–6685. http://dx.doi.org/10.1074/jbc.270.12.6678.
8. **Durell SR, Bakker EP, Guy HR.** 2000. Does the KdpA subunit from the high affinity $K^+$-translocating P-type KDP-ATPase have a structure similar to that of $K^+$ channels? Biophys J **78:**188–199. http://dx.doi.org/10.1016/S0006-3495(00)76584-2.
9. **Durell SR, Guy HR.** 1999. Structural models of the KtrB, TrkH, and Trk1,2 symporters based on the structure of the KcsA $K^+$ channel. Biophys J **77:**789–807. http://dx.doi.org/10.1016/S0006-3495(99)76932-8.
10. **Durell SR, Hao YL, Nakamura T, Bakker EP, Guy HR.** 1999. Evolutionary relationship between $K^+$ channels and symporters. Biophys J **77:**775–788. http://dx.doi.org/10.1016/S0006-3495(99)76931-6.
11. **Kato Y, Sakaguchi M, Mori Y, Saito K, Nakamura T, Bakker EP, Sato Y, Goshima S, Uozumi N.** 2001. Evidence in support of a four transmembrane-pore-transmembrane topology model for the *Arabidopsis thaliana* $Na^+/K^+$ translocating AtHKT1 protein, a member of the superfamily of $K^+$ transporters. Proc Natl Acad Sci U S A **98:**6488–6493. http://dx.doi.org/10.1073/pnas.101556598.
12. **Sato Y, Nanatani K, Hamamoto S, Shimizu M, Takahashi M, Tabuchi-Kobayashi M, Mizutani A, Schroeder JI, Souma S, Uozumi N.** 2014. Defining membrane spanning domains and crucial membrane-localized acidic amino acid residues for $K^+$ transport of a Kup/HAK/KT-type *Escherichia coli* potassium transporter. J Biochem **155:**315–323. http://dx.doi.org/10.1093/jb/mvu007.
13. **Zanetti M, Teardo E, La Rocca N, Zulkifli L, Checchetto V, Shijuku T, Sato Y, Giacometti GM, Uozumi N, Bergantino E, Szabo I.** 2010. A novel potassium channel in photosynthetic cyanobacteria. PLoS One **5:**e10118. http://dx.doi.org/10.1371/journal.pone.0010118.
14. **Checchetto V, Segalla A, Allorent G, La Rocca N, Leanza L, Giacometti GM, Uozumi N, Finazzi G, Bergantino E, Szabo I.** 2012. Thylakoid potassium channel is required for efficient photosynthesis in cyanobacteria. Proc Natl Acad Sci U S A **109:**11043–11048. http://dx.doi.org/10.1073/pnas.1205960109.
15. **Carraretto L, Formentin E, Teardo E, Checchetto V, Tomizioli M, Morosinotto T, Giacometti GM, Finazzi G, Szabo I.** 2013. A thylakoid-located two-pore $K^+$ channel controls photosynthetic light utilization in plants. Science **342:**114–118. http://dx.doi.org/10.1126/science.1242113.
16. **Hamamoto S, Uozumi N.** 2014. Organelle-localized potassium transport systems in plants. J Plant Physiol **171:**743–747. http://dx.doi.org/10.1016/j.jplph.2013.09.022.
17. **Berry S, Esper B, Karandashova I, Teuber M, Elanskaya I, Rogner M, Hagemann M.** 2003. Potassium uptake in the unicellular cyanobacterium *Synechocystis* sp. strain PCC 6803 mainly depends on a Ktr-like system encoded by slr1509 (ntpJ). FEBS Lett **548:**53–58. http://dx.doi.org/10.1016/S0014-5793(03)00729-4.
18. **Matsuda N, Kobayashi H, Katoh H, Ogawa T, Futatsugi L, Nakamura T, Bakker EP, Uozumi N.** 2004. $Na^+$-dependent $K^+$ uptake Ktr system from the cyanobacterium *Synechocystis* sp. PCC 6803 and its role in the early phases of cell adaptation to hyperosmotic shock. J Biol Chem **279:**54952–54962. http://dx.doi.org/10.1074/jbc.M407268200.
19. **Price-Whelan A, Poon CK, Benson MA, Eidem TT, Roux CM, Boyd JM, Dunman PM, Torres VJ, Krulwich TA.** 2013. Transcriptional profiling of *Staphylococcus aureus* during growth in 2 M NaCl leads to clarification of physiological roles for Kdp and Ktr $K^+$ uptake systems. mBio **4**(4):e00407-13. http://dx.doi.org/10.1128/mBio.00407-13.
20. **Grundling A.** 2013. Potassium uptake systems in Staphylococcus aureus: new stories about ancient systems. mBio **4**(5):e00784-13. http://dx.doi.org/10.1128/mBio.00784-13.
21. **Haupt M, Bramkamp M, Coles M, Kessler H, Altendorf K.** 2005. Prokaryotic Kdp-ATPase: recent insights into the structure and function of KdpB. J Mol Microbiol Biotechnol **10:**120–131. http://dx.doi.org/10.1159/000091559.
22. **Siebers A, Altendorf K.** 1989. Characterization of the phosphorylated intermediate of the $K^+$-translocating Kdp-ATPase from *Escherichia coli*. J Biol Chem **264:**5831–5838.
23. **Altendorf K, Siebers A, Epstein W.** 1992. The KDP ATPase of *Escherichia coli*. Ann N Y Acad Sci **671:**228–243. http://dx.doi.org/10.1111/j.1749-6632.1992.tb43799.x.
24. **Altendorf K, Gassel M, Puppe W, Mollenkamp T, Zeeck A, Boddien C, Fendler K, Bamberg E, Drose S.** 1998. Structure and function of the Kdp-ATPase of *Escherichia coli*. Acta Physiol Scand Suppl **643:**137–146.
25. **Gassel M, Mollenkamp T, Puppe W, Altendorf K.** 1999. The KdpF

subunit is part of the $K^+$-translocating Kdp complex of *Escherichia coli* and is responsible for stabilization of the complex in vitro. J Biol Chem **274:**37901–37907. http://dx.doi.org/10.1074/jbc.274.53.37901.
26. **Rhoads DB, Waters FB, Epstein W.** 1976. Cation transport in *Escherichia coli*. VIII. Potassium transport mutants. J Gen Physiol **67:**325–341.
27. **Xue T, You Y, Hong D, Sun H, Sun B.** 2011. The *Staphylococcus aureus* KdpDE two-component system couples extracellular $K^+$ sensing and Agr signaling to infection programming. Infect Immun **79:**2154–2167. http://dx.doi.org/10.1128/IAI.01180-10.
28. **Ballal A, Basu B, Apte SK.** 2007. The Kdp-ATPase system and its regulation. J Biosci **32:**559–568. http://dx.doi.org/10.1007/s12038-007-0055-7.
29. **Reed RH, Warr SRC, Richardson DL, Moore DJ, Stewart WDP.** 1985. Multiphasic osmotic adjustment in a euryhaline cyanobacterium. FEMS Microbiol Lett **28:**225–229. http://dx.doi.org/10.1111/j.1574-6968.1985.tb00796.x.
30. **Tholema N, Vor der Bruggen M, Maser P, Nakamura T, Schroeder JI, Kobayashi H, Uozumi N, Bakker EP.** 2005. All four putative selectivity filter glycine residues in KtrB are essential for high affinity and selective $K^+$ uptake by the KtrAB system from *Vibrio alginolyticus*. J Biol Chem **280:**41146–41154. http://dx.doi.org/10.1074/jbc.M507647200.
31. **Stumpe S, Bakker EP.** 1997. Requirement of a large $K^+$-uptake capacity and of extracytoplasmic protease activity for protamine resistance of *Escherichia coli*. Arch Microbiol **167:**126–136. http://dx.doi.org/10.1007/s002030050425.
32. **Uozumi N, Nakamura T, Schroeder JI, Muto S.** 1998. Determination of transmembrane topology of an inward-rectifying potassium channel from Arabidopsis thaliana based on functional expression in *Escherichia coli*. Proc Natl Acad Sci U S A **95:**9773–9778. http://dx.doi.org/10.1073/pnas.95.17.9773.
33. **Zulkifli L, Akai M, Yoshikawa A, Shimojima M, Ohta H, Guy HR, Uozumi N.** 2010. The KtrA and KtrE subunits are required for $Na^+$-dependent $K^+$ uptake by KtrB across the plasma membrane in *Synechocystis* sp. strain PCC 6803. J Bacteriol **192:**5063–5070. http://dx.doi.org/10.1128/JB.00569-10.
34. **Zulkifli L, Uozumi N.** 2006. Mutation of His-157 in the second pore loop drastically reduces the activity of the *Synechocystis* Ktr-type transporter. J Bacteriol **188:**7985–7987. http://dx.doi.org/10.1128/JB.00886-06.
35. **Kimura S, Shiraiwa Y, Suzuki I.** 2009. Function of the N-terminal region of the phosphate-sensing histidine kinase, SphS, in *Synechocystis* sp. PCC 6803. Microbiology **155**(Pt 7)**:**2256–2264. http://dx.doi.org/10.1099/mic.0.028514-0.
36. **Miller JH.** 1972. Experiments in molecular genetics. Cold Spring Harbor Laboratory Press, Cold Spring Harbor, NY.
37. **Kucho K, Aoki K, Itoh S, Ishiura M.** 2005. Improvement of the bioluminescence reporter system for real-time monitoring of circadian rhythms in the cyanobacterium *Synechocystis* sp. strain PCC 6803. Genes Genet Syst **80:**19–23. http://dx.doi.org/10.1266/ggs.80.19.
38. **Kondo T.** 1983. Phase-shifts of potassium uptake rhythm in *Lemna gibba* G3 due to light, dark or temperature pulses. Plant Cell Physiol **24:**659–665.
39. **Snaith PJ, Mansfield TA.** 1986. The circadian rhythm of stomatal opening: evidence for the involvement of potassium and chloride fluxes. J Exp Bot **37:**188–199. http://dx.doi.org/10.1093/jxb/37.2.188.
40. **Itri JN, Vosko AM, Schroeder A, Dragich JM, Michel S, Colwell CS.** 2010. Circadian regulation of a-type potassium currents in the suprachiasmatic nucleus. J Neurophysiol **103:**632–640. http://dx.doi.org/10.1152/jn.00670.2009.
41. **Aoki S, Kondo T, Ishiura M.** 1995. Circadian expression of the *dnaK* gene in the cyanobacterium *Synechocystis* sp. strain PCC 6803. J Bacteriol **177:**5606–5611.
42. **Mitschke J, Georg J, Scholz I, Sharma CM, Dienst D, Bantscheff J, Voss B, Steglich C, Wilde A, Vogel J, Hess WR.** 2011. An experimentally anchored map of transcriptional start sites in the model cyanobacterium *Synechocystis* sp. PCC6803. Proc Natl Acad Sci U S A **108:**2124–2129. http://dx.doi.org/10.1073/pnas.1015154108.
43. **Kato N, Akai M, Zulkifli L, Matsuda N, Kato Y, Goshima S, Hazama A, Yamagami M, Guy HR, Uozumi N.** 2007. Role of positively charged amino acids in the $M2_D$ transmembrane helix of Ktr/Trk/HKT type cation transporters. Channels (Austin) **1:**161–171. http://dx.doi.org/10.4161/chan.4374.
44. **Yang AH, Moore SD, Schmidt BS, Klug M, Lipson M, Erickson D.** 2009. Optical manipulation of nanoparticles and biomolecules in sub-wavelength slot waveguides. Nature **457:**71–75. http://dx.doi.org/10.1038/nature07593.
45. **Wakamoto Y, Ramsden J, Yasuda K.** 2005. Single-cell growth and division dynamics showing epigenetic correlations. Analyst **130:**311–317. http://dx.doi.org/10.1039/b409860a.
46. **Peng CC, Liao WH, Chen YH, Wu CY, Tung YC.** 2013. A microfluidic cell culture array with various oxygen tensions. Lab Chip **13:**3239–3245. http://dx.doi.org/10.1039/c3lc50388g.
47. **Gomez-Sjoberg R, Leyrat AA, Pirone DM, Chen CS, Quake SR.** 2007. Versatile, fully automated, microfluidic cell culture system. Anal Chem **79:**8557–8563. http://dx.doi.org/10.1021/ac071311w.
48. **Kim MJ, Lee SC, Pal S, Han E, Song JM.** 2011. High-content screening of drug-induced cardiotoxicity using quantitative single cell imaging cytometry on microfluidic device. Lab Chip **11:**104–114. http://dx.doi.org/10.1039/c0lc00110d.
49. **Marin K, Stirnberg M, Eisenhut M, Kramer R, Hagemann M.** 2006. Osmotic stress in *Synechocystis* sp. PCC 6803: low tolerance towards nonionic osmotic stress results from lacking activation of glucosylglycerol accumulation. Microbiology **152**(Pt 7)**:**2023–2030. http://dx.doi.org/10.1099/mic.0.28771-0.
50. **Fishov I, Woldringh CL.** 1999. Visualization of membrane domains in Escherichia coli. Mol Microbiol **32:**1166–1172. http://dx.doi.org/10.1046/j.1365-2958.1999.01425.x.
51. **Alahari A, Ballal A, Apte SK.** 2001. Regulation of potassium-dependent Kdp-ATPase expression in the nitrogen-fixing cyanobacterium *Anabaena torulosa*. J Bacteriol **183:**5778–5781. http://dx.doi.org/10.1128/JB.183.19.5778-5781.2001.
52. **Laimins LA, Rhoads DB, Epstein W.** 1981. Osmotic control of kdp operon expression in *Escherichia coli*. Proc Natl Acad Sci U S A **78:**464–468. http://dx.doi.org/10.1073/pnas.78.1.464.
53. **Ballal A, Apte SK.** 2005. Differential expression of the two kdp operons in the nitrogen-fixing cyanobacterium *Anabaena* sp. strain L-31. Appl Environ Microbiol **71:**5297–5303. http://dx.doi.org/10.1128/AEM.71.9.5297-5303.2005.
54. **Ballal A, Heermann R, Jung K, Gassel M, Apte SK, Altendorf K.** 2002. A chimeric *Anabaena/Escherichia coli* KdpD protein (Anacoli KdpD) functionally interacts with E-coli KdpE and activates kdp expression in *E. coli*. Arch Microbiol **178:**141–148. http://dx.doi.org/10.1007/s00203-002-0435-1.
55. **Katoh H, Asthana RK, Ohmori M.** 2004. Gene expression in the *cyanobacterium Anabaena* sp. PCC7120 under desiccation. Microb Ecol **47:**164–174. http://dx.doi.org/10.1007/s00248-003-1043-6.
56. **Tsunekawa K, Shijuku T, Hayashimoto M, Kojima Y, Onai K, Morishita M, Ishiura M, Kuroda T, Nakamura T, Kobayashi H, Sato M, Toyooka K, Matsuoka K, Omata T, Uozumi N.** 2009. Identification and characterization of the $Na^+/H^+$ antiporter Nhas3 from the thylakoid membrane of *Synechocystis* sp. PCC 6803. J Biol Chem **284:**16513–16521. http://dx.doi.org/10.1074/jbc.M109.001875.
57. **Akai M, Onai K, Morishita M, Mino H, Shijuku T, Maruyama H, Arai F, Itoh S, Hazama A, Checchetto V, Szabo I, Yukutake Y, Suematsu M, Yasui M, Ishiura M, Uozumi N.** 2012. Aquaporin AqpZ is involved in cell volume regulation and sensitivity to osmotic stress in *Synechocystis* sp. strain PCC 6803. J Bacteriol **194:**6828–6836. http://dx.doi.org/10.1128/JB.01665-12.
58. **Nanatani K, Shijuku T, Akai M, Yukutake Y, Yasui M, Hamamoto S, Onai K, Morishita M, Ishiura M, Uozumi N.** 2013. Characterization of the role of a mechanosensitive channel in osmotic down shock adaptation in *Synechocystis* sp PCC 6803. Channels (Austin) **7:**238–242. http://dx.doi.org/10.4161/chan.25350.
59. **Dong G, Yang Q, Wang Q, Kim YI, Wood TL, Osteryoung KW, van Oudenaarden A, Golden SS.** 2010. Elevated ATPase activity of KaiC applies a circadian checkpoint on cell division in *Synechococcus elongatus*. Cell **140:**529–539. http://dx.doi.org/10.1016/j.cell.2009.12.042.
60. **Sweeney BM.** 1974. The potassium content of *Gonyaulax polyedra* and phase changes in the circadian rhythm of stimulated bioluminescence by short exposures to ethanol and valinomycin. Plant Physiol **53:**337–342. http://dx.doi.org/10.1104/pp.53.3.337.
61. **Escassi L, Aguilera J, Figueroa FL, Fernandez JA.** 2002. Potassium drives daily reversible thallus enlargement in the marine red alga *Porphyra leucosticta* (Rhodophyta). Planta **214:**759–766. http://dx.doi.org/10.1007/s004250100669.
62. **Chen ZH, Hills A, Baetz U, Amtmann A, Lew VL, Blatt MR.** 2012. Systems dynamic modeling of the stomatal guard cell predicts emergent behaviors in transport, signaling, and volume control. Plant Physiol **159:**1235–1251. http://dx.doi.org/10.1104/pp.112.197350.

63. **Moshelion M, Becker D, Czempinski K, Mueller-Roeber B, Attali B, Hedrich R, Moran N.** 2002. Diurnal and circadian regulation of putative potassium channels in a leaf moving organ. Plant Physiol **128:**634–642. http://dx.doi.org/10.1104/pp.010549.
64. **Simonetta SH, Romanowski A, Minniti AN, Inestrosa NC, Golombek DA.** 2008. Circadian stress tolerance in adult *Caenorhabditis elegans*. J Comp Physiol A Neuroethol Sens Neural Behav Physiol **194:**821–828. http://dx.doi.org/10.1007/s00359-008-0353-z.
65. **Alahari A, Apte SK.** 1998. Pleiotropic effects of potassium deficiency in a heterocystous, nitrogen-fixing cyanobacterium, *Anabaena torulosa*. Microbiology **144**(Pt 6)**:**1557–1563. http://dx.doi.org/10.1099/00221287-144-6-1557.
66. **Okamoto K, Onai K, Ishiura M.** 2005. RAP, an integrated program for monitoring bioluminescence and analyzing circadian rhythms in real time. Anal Biochem **340:**193–200. http://dx.doi.org/10.1016/j.ab.2004.11.007.